Published in partnership with Beijing Technology and Business University & International Union of Food Science and Technology



https://doi.org/10.1038/s41538-025-00500-0

Qualitative analysis of edible oil mixture for omega-3 content using terahertz time-domain spectroscopy



Lan-Hee Yang¹, Inhee Maeng¹, Sanggu Lee¹, Kwangsung Kim², Young Bin Ji³, Hyeon Sang Bark³, Hee Jun Shin⁴⊠ & Seung Jae Oh¹⊠

The utility of terahertz time-domain spectroscopy (THz-TDS) for the qualitative and quantitative analysis of edible oils remains underexplored. Therefore, we aimed to characterize an edible oil mixture consisting of perilla, soybean, and corn oils using THz-TDS spectroscopy and compare the findings with those from Fourier transform infrared spectroscopy (FT-IR) and proton nuclear magnetic resonance (¹H NMR) spectroscopy. THz-TDS was used to obtain complex optical constants such as power absorption and refractive index of oils in the range of 0.2–2.0 THz. Perilla oil mixtures were quantitatively analyzed using complex dielectric constants in the THz frequency region. We characterized the double bond structure of omega-3 in perilla oil using THz-TDS. Furthermore, we used reflection-mode THz-TDS imaging to demonstrate its application as a non-destructive authenticity test for bottled edible oil.

Edible oils are a vital source of essential nutrients for the human body. Vegetable oils are primarily composed of saturated fatty acids, monounsaturated fatty acids such as omega-9 fatty acids, and polyunsaturated fatty acids such as omega-3 and omega-6 fatty acids. Omega-3 fatty acids help reduce neutral fat levels, improve vascular function, and offer other benefits, such as preventing Alzheimer's disease and inhibiting cancer cell proliferation¹⁻³. Mammals cannot synthesize alpha-linolenic acid (ALA), an essential plant-based omega-3 fatty acid. Hence, unlike docosahexaenoic acid (DHA) and eicosapentaenoic acid (EPA), ALA must be obtained from dietary sources such as vegetable oils. ALA constitutes over 60% of the total fatty acid components of perilla oil, a common edible vegetable oil extracted from perilla seeds⁴. Owing to the high proportion of ALA, there is a growing demand for perilla oil for health purposes, necessitating the development of techniques for quality assessment and extraction of high-purity perilla oil. Although commercially available perilla-flavored oil typically comprises 15% perilla oil and 70% soybean oil, consumers rarely discern the purity of oils based solely on flavor. Such products may be fraudulently marketed as high-purity perilla oil, misrepresenting their composition. Unlike fatty acids, which are mostly composed of single bonds, unsaturated fatty acids contain double bonds (Fig. 1). Measuring these double bonds is a key technique that enables qualitative and quantitative analyses of edible oils with omega-3 fatty acid content similar to that of perilla oil.

Traditional methods for detecting oil adulteration, such as gas chromatography (GC), high-performance liquid chromatography (HPLC), nuclear magnetic resonance (NMR), and Fourier-transform infrared spectroscopy (FT-IR), are highly accurate but limited by high cost, complex procedures, long analysis times, and the inability to perform real-time or onsite analysis. Several methods, such as NMR^{5,6} and FT-IR^{7,8} spectroscopy, have been employed to qualify and quantify the purity of omega-3 fatty acids by analyzing their molecular structure9. NMR techniques provide accurate structural analysis but require complex pre- and post-processing steps. FT-IR spectroscopy captures the binding structure or motion of molecules that lie in the infrared spectrum of material absorption but requires sample processing and post-analysis, such as the Kramers-Kronig transformation, to obtain complex dielectric constants. However, as both these techniques are challenging to implement in user-friendly, portable systems for market or industrial applications, a novel technology is required to enable simple and conclusive measurements to authenticate perilla oil, while ensuring both accuracy and portability.

Terahertz (THz) wave technology, which uses electromagnetic waves with wavelengths between 3 mm and 30 μ m (energies of a few meV) have been regarded as novel non-destructive inspection testing technique for foods, semiconductor, medicine and so one, because of safety of human body and high transmission properties. THz spectroscopy has been used as

¹YUHS-KRIBB Medical Convergence Research Institute, College of Medicine, Yonsei University, Seoul, 03722, Republic of Korea. ²DADream gristmill, Cheorwongun, Gangwon-do, 24031, Republic of Korea. ³Division of Applied Photonics System Research, Advanced Photonics Research Institute (APRI), Gwangju Institute of Science and Technology (GIST), Gwangju, 61005, Republic of Korea. ⁴Pohang Accelerator Laboratory, POSTECH, Pohang, 37673, Republic of Korea. ⊠e-mail: shinhj@postech.ac.kr; issac@yuhs.ac

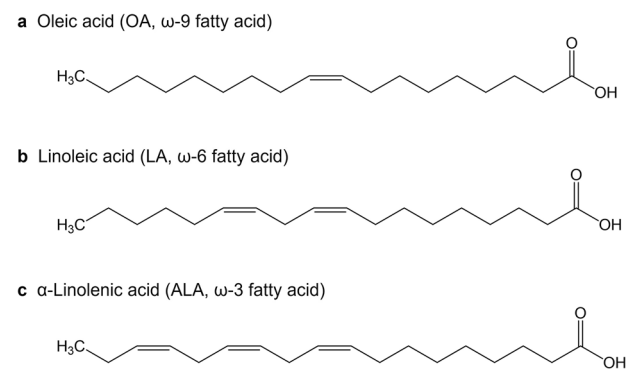


Fig. 1 | Molecular structures of unsaturated fatty acids. a oleic acid (OA, $C_{18}H_{34}O_2$, ω -9 fatty acid), b linoleic acid (LA, $C_{18}H_{32}O_2$, ω -6 fatty acid), and c alphalinolenic acid (ALA, $C_{18}H_{30}O_2$, ω -3 fatty acid).



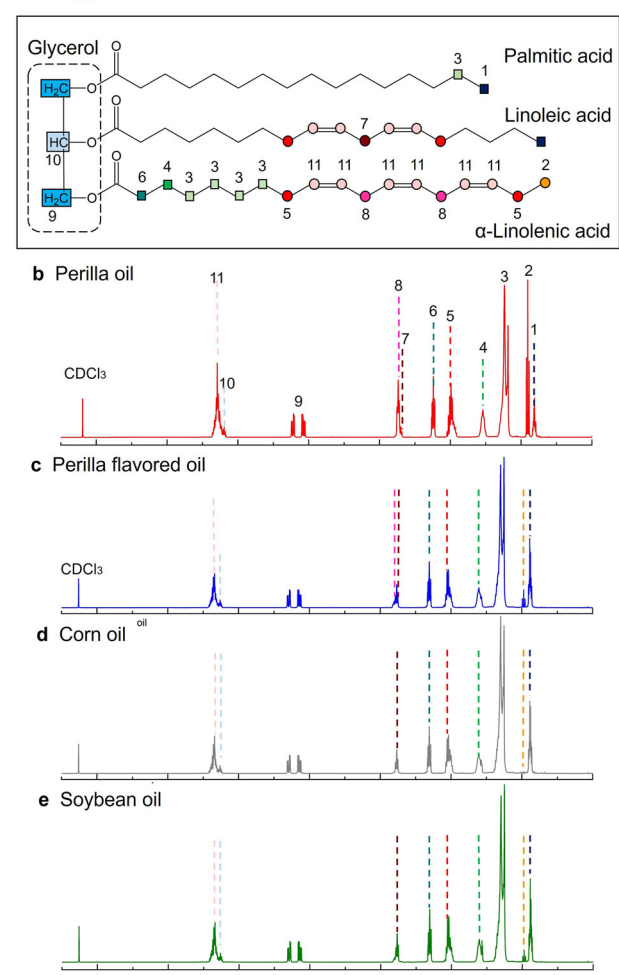


Fig. 2 | Triglyceride structure and 1H NMR spectrum of various edible oils (perilla oil, perilla flavored oil, corn oil, and soybean oil). a Triglyceride structure composed of palmitic acid, linoleic acid, and α -linolenic acid and symbol display of fatty acid functional group for each signal of 1 H NMR spectrum. 1 H NMR spectra of **b** perilla oil, **c** perilla flavored oil, **d** corn oil, and **e** soybean oil.

Chemical Shift (ppm)

an analytical method for studying the molecular structure and dynamics of materials, such as semiconductors¹⁰, polymers¹¹, foods^{12,13} and liquid mixtures^{14,15}. Several physical and optical parameters, such as the phonon frequency, recombination energy of large molecules, and weak hydrogen

bonds, can be used to characterize materials in the THz frequency range^{16,17}. Biomolecular structures, such as the single- and double-stranded structures of deoxyribonucleic acid (DNA) and the single- and triple-stranded helices of β-glucans in laminarin have been identified using THz wave spectroscopy^{18,19}. The dielectric response of liquids within the THz frequency range, which is attributable to intramolecular interactions resulting from the collective or recombination motion of liquid molecules, reflects the polarity of liquids. Both polar²⁰ and nonpolar²¹ liquids, such as alcohols and oils, and their mixtures²² can be differentiated and qualified using THz spectroscopy. THz time-domain spectroscopy (THz-TDS), in which THz electromagnetic fields are measured to output amplitude and phase information directly, enables the extraction of complex refractive properties and dielectric constants without a fitting process such as the Kramers-Kronig transformation needed in FT-IR spectroscopy. Thus, THz-TDS has emerged as a viable analytical technique for identifying impurities and denaturation in oils.

Although THz-TDS studies on fuel^{23–25} and edible^{26,27} oils have been reported previously, most have focused on determining the THz optical properties of oils and rancid oils. A few studies, such as those by Gorenflo et al.²⁸ and Abdul-Munaim et al.²⁹, have also investigated oil–water mixtures. However, studies on oil–oil mixtures have rarely been reported, despite their necessity to understand oil-oil interactions and purification.

In this study, we aimed to characterize mixtures of perilla oil with other oils using FT-IR, proton NMR (¹H NMR) spectroscopy, and transmission-and reflection-mode THz-TDS. The concentrations of perilla oil in mixtures containing soybean and corn oil were characterized by analyzing the complex dielectric constants extracted via THz-TDS. Reflection-mode THz-TDS, which allows the real-time measurement of THz signals, was used to demonstrate its potential as a non-contact method for authenticity testing of perilla oil and determining omega-3 content.

Results 1H NMR spectroscopy

Vegetable cooking oil mainly exists in the form of triglyceride (Fig. 2a), and is composed of three of the unsaturated and saturated fatty acids within the glycerol molecule ($C_3H_8O_3$) through ester bonds. In addition, edible oils are composed of more than 80% of unsaturated fatty acids, namely, oleic acid (OA, $C_{18}H_{34}O_2$, ω -9 fatty acid), linoleic acid (LA, $C_{18}H_{32}O_2$, ω -6 fatty acid), and alpha-linolenic acid (ALA, $C_{18}H_{30}O_2$, ω -3 fatty acid). As shown in Fig. 1, they share a common hydrocarbon chain structure with 18 carbons; however, the numbers of single and double bonds between the carbons differ. Generally, GC is used for fatty acid analysis, but the relative contents of the three unsaturated fatty acids and all saturated fatty acids can be simply calculated by obtaining the integral value of the signal corresponding to the fatty acid functional group through NMR spectroscopy⁵. Figure 2 (b, c, d, and e) shows the ¹H NMR spectra of perilla oil, perilla flavored oil, corn oil, and soybean oil in CDCl₃ and indicates the fatty acid functional group corresponding to each signal.

Table 1 shows the nutrient content of perilla oil⁴, corn oil³⁰, and soybean oil³¹ obtained through the GC method conducted in other literature, and the fatty acid content analyzed through ¹H NMR spectroscopy of the oils used in in this experiment.

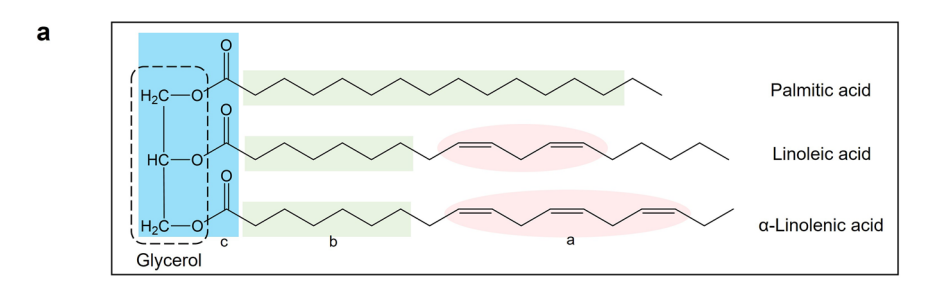
ALA content was calculated from the methyl group peaks on both fatty acids and unsaturated fatty acids. The peak representing the methyl group in ALA appeared in the range of 0.96–0.88 ppm (signal 2 in Fig. 2), while the methyl peaks of fatty acid, LA and OA appeared in the range of 0.86–0.78 ppm (signal 1 in Fig. 2). LA content was obtained by subtracting the ALA value from the integral value of 2.73–2.84 ppm (signals 7 and 8 in Fig. 2), which is the hydrogen signal between double bonds among the integral values of all fatty acids (2.27–2.67 ppm, signal 6 in Fig. 2). OA was gained by subtracting the values of LA and ALA from the integral value in the range of 1.96–2.14 ppm (signal 5 in Fig. 2), which corresponds to all unsaturated fatty acids among all fatty acids. Finally, saturated fatty acids were estimated by excluding the total unsaturated fatty acid content.

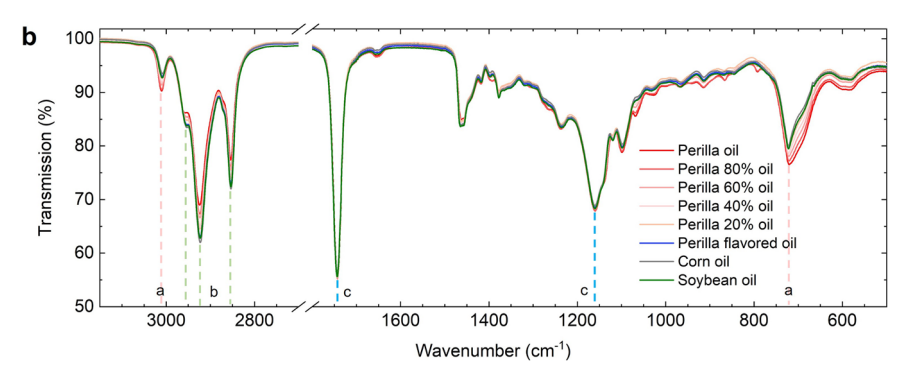
Table 1 | Nutritional content of edible oils (Perilla oil, perilla flavored oil, corn oil, and soybean oil)

Type of oil	Saturated fatty acids	Monounsaturated fatty acids Oleic acid (C18:1, ω-9)	Polyunsaturated fatty acids Linoleic acid (C18:2, ω-6)	α-Linolenic acid (C18:3, ω-3)	Ref, method
Perilla oil	6–10	14–23	11–16	54–64	Ref. 4, GC
	11.6	12.2	17.7	58.5	This study, ¹ H NMR
Perilla flavored oil	17.8	24.8	45.8	11.9	This study, ¹ H NMR
Corn oil	12.9	27.3	58	1	Ref. 30, GC
	16.6	34.1	45.7	3.6	This study, ¹ H NMR
Soybean oil	15.6	22.6	51	7	Ref. 31, GC
	18.2	23.6	50.2	8.0	This study, ¹ H NMR

The values are expressed as percent (%).

Fig. 3 | Triglyceride structure and FT-IR spectrum of various edible oils (perilla oil, perilla flavored oil, corn oil, and soybean oil) and perilla oil mixtures (80, 60, 40, 20%). a Triglyceride structure composed of palmitic acid, linoleic acid, and α -linolenic acid and symbol display of fatty acid functional group for frequency band of Fourier transform infrared spectra. FT-IR spectra of **b** perilla oil, perilla flavored oil, perilla oil mixtures (80, 60, 40, 20%), corn oil, and soybean oil.





Only perilla oil, which has a high content of ALA with three C=C bonds, showed high intensity as a characteristic indicator in the range of 5.35 ppm and 2.80 ppm (signals 11 and 8 in Fig. 2) and the range of 0.96–0.88 ppm (signal 2 in Fig. 2) of the methyl group of ALA. Thus, ALA is suitable as a marker for perilla oil mixtures. The integral values of signal 2 for perilla oil, perilla flavored oil, corn oil, and soybean oil were 9.32, 2.01, 0.67, and 1.25, respectively. In contrast, the spectra of perilla flavored oil, corn oil, and soybean oil were higher than that of perilla oil in the range 1.31–1.25 ppm (signal 3 in Fig. 2), owing to the presence of a greater number of single bonds.

FT-IR spectroscopy

FT-IR spectroscopy was employed to analyze perilla oil, perilla flavored oil, soybean oil, and corn oil (Fig. 3b), with their corresponding triglyceride structures presented in Fig. 3a. Furthermore, binary mixtures of perilla and soybean oils at varying concentrations (20%, 40%, 60%, and 80%) were examined to elucidate compositional differences. Although commercial products typically contain less than 20% perilla oil due to its relatively high cost, higher blending ratios were included in this study to systematically investigate the effect of ALA content on the THz spectral response.

The absorption band observed at $3008-3010~{\rm cm}^{-1}$ corresponds to the cis-double bond stretching vibration of C = C–H in unsaturated fatty acids. Notably, perilla oil, which contains a high concentration of ALA, exhibited an increased absorption intensity at this band, indicating a higher degree of unsaturation.

While the $720~cm^{-1}$ peak is generally attributed to CH_2 rocking vibrations, the presence of cis-disubstituted olefins in ALA appears to influence the out-of-plane deformation mode, leading to an enhanced intensity of bands below $720~cm^{-1}$. This suggests that ω -3 rich oils exhibit distinct vibrational characteristics due to their molecular configuration.

The transmission peaks at $2853~\text{cm}^{-1}$; and $2923~\text{cm}^{-1}$ (region b) arise from the methylene (-CH₂-) stretching vibrations in the alkane chains of fatty acids. A progressive increase in transmission intensity at these bands was observed with the increasing proportion of perilla oil, further reflecting the compositional influence of ALA.

In the carbonyl region (c), the 1743 cm $^{-1}$ peak is assigned to the ester carbonyl (-C = O) stretching vibration in triglycerides, a characteristic feature of lipids and fatty acids. Additionally, the peaks at $1160\,\rm cm^{-1}$ and $1090\,\rm cm^{-1}$ correspond to C–O and C–O–C stretching vibrations in triglycerides, exhibiting similar spectral patterns across all samples.

The FT-IR spectrum results of unsaturated fatty acids can be effectively differentiated by comparing the spectral variations associated with double and single carbon bonds, analogous to ¹H NMR spectroscopy. The progressive increase in transmission intensity at 2853 cm⁻¹ and 2923 cm⁻¹, as well as the sequential decrease in the 720 cm⁻¹ peak with increasing perilla oil content with high ALA, highlights the efficacy of FT-IR and ¹H NMR spectroscopy in distinguishing perilla oil from other edible oils.

Transmission-mode THz-TDS experiment

The THz time-domain waveforms of perilla oil, soybean oil, corn oil, perilla flavored oil, and perilla oil mixed oils are shown in Fig. 4. The THz pulse amplitudes of corn oil and soybean oil were higher than those of the other oils, including perilla oil. The pulse of perilla oil exhibited a temporal delay compared to that of soybean and corn oils. As the concentration of perilla oil increased, the amplitude of the THz pulse decreased, and the peak position was delayed. This implies that the complex refractive indices, such as the power absorption and refractive index, of perilla oil were larger than those of soybean and corn oils.

The absorption coefficients and refractive indices of perilla oil, soybean oil, corn oil, and their mixtures were measured in the range of 0.2–2.0 THz

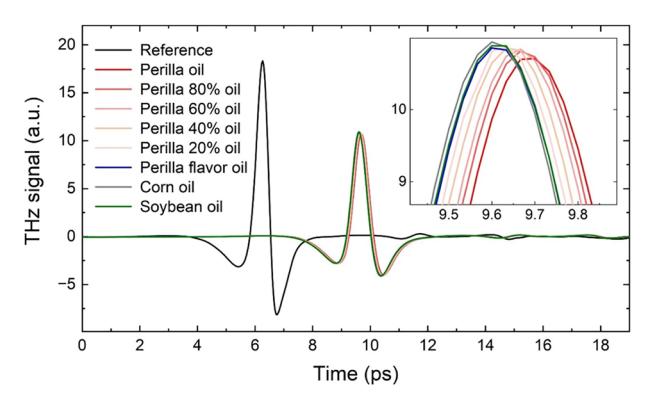


Fig. 4 | THz time-domain waveforms of perilla oil, perilla flavored oil, soybean oil, corn oil and their mixtures.

(Fig. 5a, b). Among the oils, perilla oil exhibited the highest absorption coefficients and refractive indices, followed by soybean oil and corn oil. At 1.0 THz, perilla oil showed a refractive index of approximately 1.517 and an absorption coefficient of about 9.960 cm⁻¹, both of which varied consistently with frequency. Furthermore, as the perilla oil concentration increased in the mixtures, both the refractive index and absorption power increased accordingly (Fig. 5c). The concentration of perilla oil showed a strong linear correlation with both the refractive index and absorption coefficient in the THz region, with Pearson correlation coefficients of 0.997 and 0.987, respectively. The standard deviation between the measured values and their linear fitting curves at 1.0 THz was 2.91% for the refractive index and 6.05% for the absorption coefficient, which could be regarded as the detection sensitivity for perilla oil using THz-TDS. The unique spectral signatures of the oils were identified using the real and imaginary parts of the dielectric constants, and the dielectric trace depicted by the imaginary dielectric constants dependent on the real dielectric constants, can thus be used to identify the oil mixtures (Fig. 5d).

These differences are closely linked to the molecular structure of α -linolenic acid (ALA), the major component of perilla oil. ALA contains multiple cis double bonds that induce bends in the hydrocarbon chain, resulting in a more flexible and non-linear molecular structure. This bent geometry facilitates delocalization of π -electrons, forming an extended π -electron cloud that enhances molecular polarizability. Consequently, larger dipole moment fluctuations occur under THz excitation, leading to stronger coupling with low-frequency vibrational modes and thus higher THz absorption. Supporting this interpretation, 1 H NMR data confirmed that soybean and corn oils contain significantly lower ALA content than perilla oil, indicating fewer double-bond structures. Similarly, FT-IR spectroscopy (Fig. 3) showed more intense unsaturation-related peaks in perilla oil-rich mixtures, correlating with higher THz refractive indices and absorption

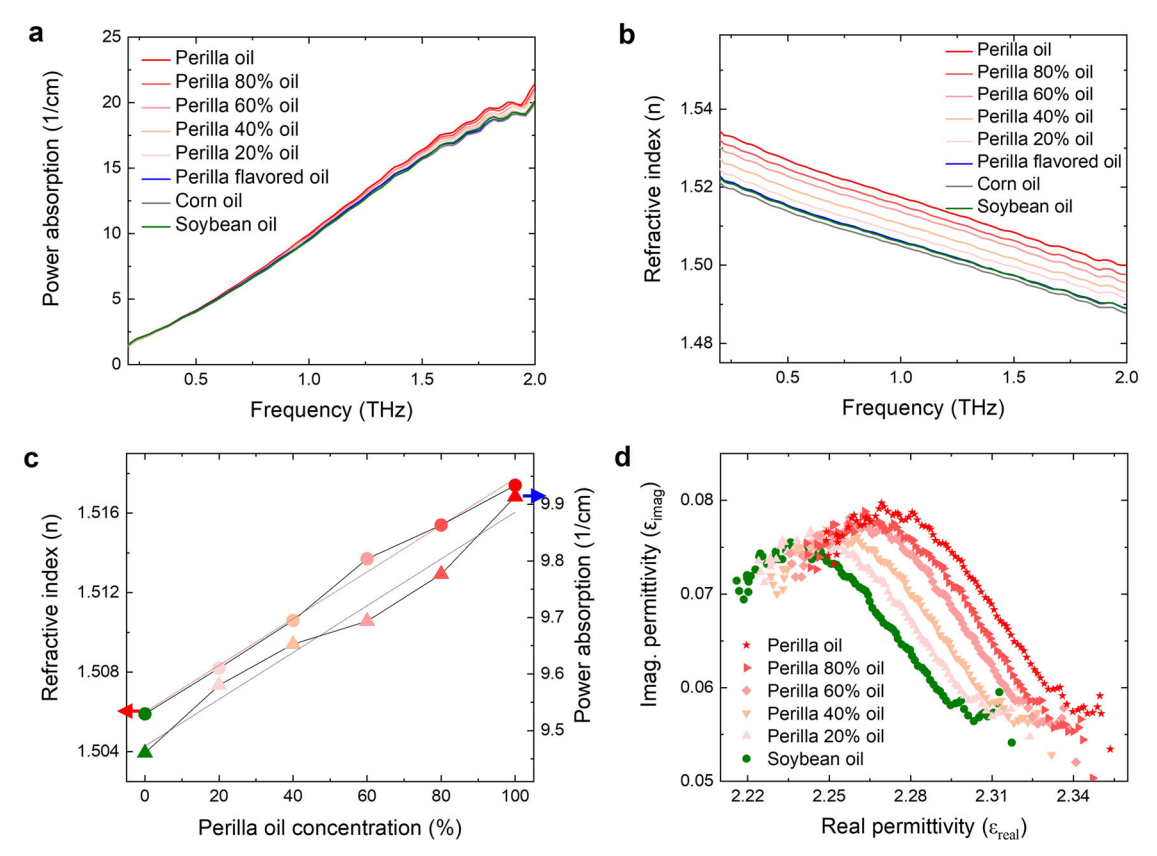
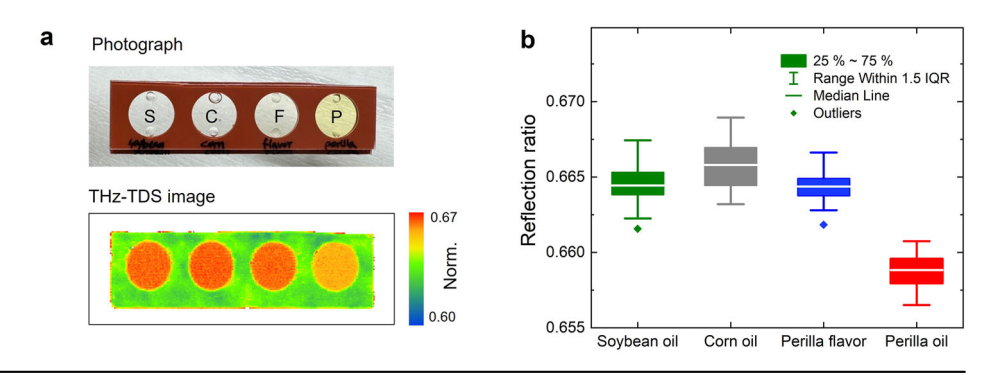


Fig. 5 | THz optical properties of edible oils and perilla oil mixtures: absorption, refractive index, and dielectric constants. a Power absorption and b refractive indices of perilla oil, soybean oil, corn oil and their mixtures, c power absorption

(triangles) and refractive indices (circles) at 1.0 THz with linear fitting line depending on perilla oil concentrations, and **d** complex dielectric constant traces at various perilla oil concentrations.

Fig. 6 | Reflection-mode THz imaging and intensity analysis of edible oils. a Photograph of the hybridization chamber and THz-TDS image of reflection mode of soybean oil (S), corn oil (C), perilla flavored oil (F) and perilla oil (P).

b Histogram of THz reflection intensity in the ROI for each oil.



coefficients. These results collectively demonstrate that THz-TDS is a powerful, non-destructive tool for characterizing edible oils and quantitatively assessing omega-3 fatty acid content through molecular-level differences in electronic and structural properties.

Reflection-mode THz-TDS imaging experiment

The transmission THz-TDS experiment showed that the THz-TDS technique can be used as a non-destructive inspection method for edible oils. However, because the products are typically bottled when brought to the market, a real-time reflection-mode system must be utilized to implement a practical non-destructive testing system. In the reflection-mode THz-TDS, the brightness of the THz image was lowest for perilla oil, whereas those of the other oils were comparable to each other (Fig. 6a). For further analysis, a histogram of the oils in the region of interest (ROI), a 5×5 mm² square was generated in Fig. 6b. Perilla oil showed the lowest reflectance values compared to soybean, perilla flavored, and corn oils. Soybean and perilla flavored oils exhibited similar values, whereas corn oil showed slightly higher reflectance values. These results corresponded to the complex constant results observed by transmission-mode THz-TDS. The differences in the refractive indices of perilla oil and the sapphire window were lower than that between soybean, corn, or perilla flavored oils (primarily composed of soybean and corn oils) and the sapphire window. This result shows that THz imaging can distinguish even minor differences between soybean and corn oils, demonstrating that THz-TDS can be used as a novel non-destructive inspection technique and that reflection-mode THz-TDS can be employed as a non-contact method for authenticating perilla oil in real markets, such as bottled oils.

Discussion

While THz-TDS has been applied to the analysis of various materials including semiconductors and biological substances, its potential in characterizing edible oils, particularly oil-oil mixtures, has been insufficiently explored. Previous studies predominantly focused on oil-water mixtures or rancidity detection. However, given the prevalence of adulterated perilla oil products in the market, a practical, non-destructive tool for compositional analysis and authenticity verification remains a significant unmet need. This study revealed that THz-TDS is capable of detecting compositional changes in perilla oil mixtures based on variations in refractive index and absorption coefficients. Oils with higher ALA content (>60%), such as pure perilla oil, exhibited higher absorption and refractive indices in the 0.2-2.0 THz range. These results were consistent with findings from ¹H NMR and FT-IR spectroscopy, both of which demonstrated unique spectral features correlated with the amount of unsaturated fatty acids. Reflection-mode THz-TDS imaging successfully discriminated between bottled perilla oil and its mixtures, confirming the feasibility of non-contact analysis in real market. The increased THz absorption and refractive index of ALA rich oil are consistent with previous spectroscopic studies on biomolecules^{18,19}. Several groups have reported that biomolecules with multiple bonds, such as doublestranded DNA and triple-helical β-glucans, exhibited higher THz absorption and refractive indices compared to single-stranded biomolecules. The response of THz signals was attributed primarily to the increased intramolecular and intermolecular interactions arising from molecular conformations. In this study, oils with a higher number of C = C double bonds (ALA-rich perilla oil) displayed stronger absorption and higher refractive indices in the THz region compared to oils such as soybean and corn oils. Our results confirm that the number of C = C double bonds in unsaturated fatty acids directly influences the optical response in the THz range. Unlike NMR and FT-IR methods that require a sample preprocessing or numerical approximation of Kramers-Kronig relations, THz-TDS offers a direct and efficient methods to obtain dielectric properties, facilitating realtime analysis. User-friendly potable THz imaging devices based on reflection type could be widely applied in industrial or retail environments. Expanding the spectral database to include a variety of edible oils could enhance the robustness and versatility of the technique in food authentication and quality control. Machine learning models employing big data of THz-TDS could improve classification accuracy and enable automated detection of oil adulteration.

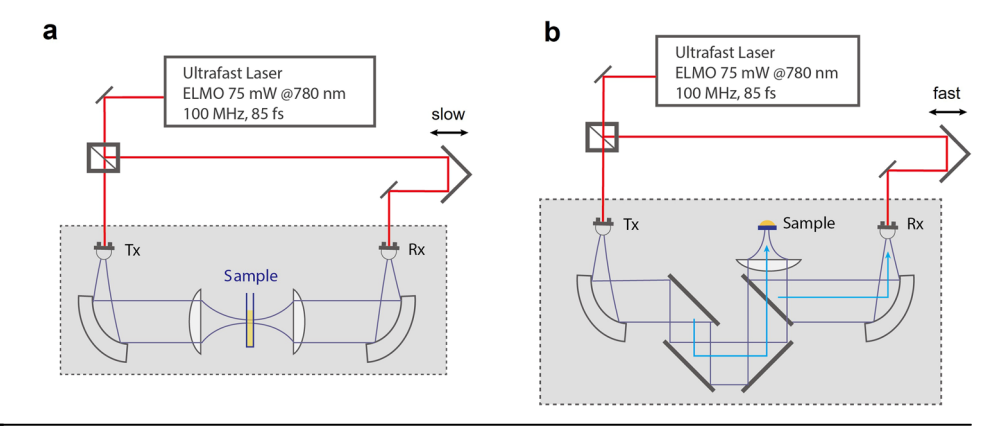
Overall, this study demonstrated that THz-TDS is an effective analytical technique for qualitative and quantitative assessment of edible oil mixtures, particularly for verifying the authenticity and omega-3 fatty acid content of perilla oil mixtures. The complex refractive indices and absorption coefficients obtained through THz-TDS were correlated with the ALA content, reflecting variations in molecular complexity due to double-bond structures in unsaturated fatty acids. Comparative analyses using ¹H NMR and FT-IR spectroscopy confirmed the reliability and accuracy of THz-TDS findings, with each technique providing complementary insights into the molecular composition of edible oils. ALA rich oils exhibited higher refractive indices and THz absorption, consistent with previous research indicating enhanced spectral responses in biomolecules with greater structural complexity. Reflection-mode THz-TDS successfully differentiated pure perilla oil from its mixtures, highlighting its potential as a practical, non-destructive method for real-time authenticity testing in commercial and industrial settings. Despite the analytical advantages of THz-TDS in detecting oil purity and composition, few limitations must be considered for industrial implementation. They include relatively high instrumentation cost, challenges in large-scale integration, and the need for regulatory validation for use in food quality assurance. Future work should address these issues to facilitate the broader adoption of THz spectroscopy in food industry applications.

Methods

Oils and sample preparation for perilla oil mixtures

Perilla oil (100%) was prepared using only perilla seeds harvested in Chulwon without any additives, including preservatives. Perilla seeds were roasted at 165–170 °C for 20 min on a pan pre-heated to 250 °C. After cooling for 5 min, the roasted seeds were pressed under 6 ton pressure to extract the oil. Soybean and corn oils (100% each) were obtained from Sajohaepyo. Perilla flavored oil (soybean oil, 71.4%; perilla extract, 14.0%; corn oil, 13.7%; and sunflower oil, 0.9%) was purchased from CJ Clean Food. Chloroform-d (99.8 atom % D) was purchased from Sigma-Aldrich. Perilla oil mixtures were prepared by blending perilla oil at different ratios (20%, 40%, 60%, and 80%) with soybean oil.

Fig. 7 | Scheme of THz-TDS systems for transmission and reflection modes. a Transmission-mode and b reflection-mode system.



Characterization by ¹H NMR and FT-IR spectroscopy

 1 H NMR spectra of the samples were recorded using a 400 MHz NMR spectrometer (AVANCE III HD 400, Bruker) with CDCl₃ as the solvent. The infrared spectra of the perilla oil mixtures were detected using Spectrum Two FT-IR spectroscopy (PerkinElmer).

THz-TDS (transmission mode and reflection mode)

All experiments were independently performed twice, and each measurement was conducted in duplicate. The reported values represent the average of the two measurements. Two types of THz-TDS methods, transmission mode and reflection mode, were used to characterize the perilla oil samples under controlled conditions (20 °C, <1% humidity). THz pulses were generated and detected using a photoconductive antenna (PCA) fabricated on low-temperature-grown (LT) GaAs. We used a femtosecond laser to induce free carriers in the PCA. The femtosecond laser had a pulse width of 85 fs, center wavelength of 780 nm, and repetition rate of 100 MHz. In transmission mode THz-TDS, the generated THz pulses were guided by two parabolic mirrors (Fig. 7a). Two TPX (Polymethylpentene) lenses of focal length 100 mm were placed between the parabolic mirrors to focus the THz pulses onto a 1 mm thick quartz cuvette with a path length of 1 mm. Timedomain pulses were then obtained using a pump-probe technique to measure the convoluted signals of the THz and probe laser pulses while varying the time delay. A slow translation stage was used in the transmission-mode system to delay the optical path. A lock-in amplifier and chopper were used to acquire THz signals with high signal-to-noise ratio.

Reflection-mode THz-TDS imaging based on a fast-delay stage was implemented to demonstrate its potential as a novel edible oil inspection method. THz images were obtained from real-time THz signals acquired via raster scanning of the sample. A low-noise current-free amplifier and data acquisition (DAQ) board were used to detect the THz signals. A fast delay stage was used with a scanning frequency and range of 20 Hz and 25 ps, respectively. In reflection-mode THz-TDS, we replaced the two TPX lenses with a reflection module consisting of three metal mirrors, a silicon beam splitter, and a TPX lens (Fig. 2b). The generated THz pulses were guided by three metal mirrors and silicon beam splitter to be focused onto the sample using a TPX lens. The oil samples were dropped onto a sapphire window, and the reflected THz pulses from the sample were guided to the PCA detector through the TPX lens, Si beam splitter, and parabolic mirror.

The four edible oils, soybean, corn, perilla flavored, and perilla, were placed in hybridization chambers attached to a sapphire window (Fig. 2a). The diameter and depth of the hybridization chambers were 9 mm and 0.5 mm, respectively. The sapphire window had a crystal axis of [100], diameter of 3 inches, and thickness of 2 mm. The reflection was determined by the refractive index mismatch at the interface between two materials. We used sapphire (with a refractive index of 3.4 in THz region) from 0.2 THz to 3 THz. The THz image was obtained by raster scanning the sapphire window with

the hybridization chamber. The image scan range was $61 \times 20 \text{ mm}^2$ with a step resolution of 0.25 mm, and it lasted around 17 min. We measured the peak-to-peak (p-p) values of the reflected time-domain waveforms, and all the p-p values of the image were divided by the p-p value reflected by the sapphire-air interface for normalization.

The acquired time-domain waveforms were converted to frequency-domain waveforms using fast Fourier transformation to obtain the frequency-dependent complex refractive properties. Accordingly, the differences in the frequency-dependent amplitude and phase, with and without the sample, represented the complex refractive properties, namely, power absorption coefficient, refractive index and complex dielectric constant, respectively.

When we consider that samples are placed in a quartz cuvette, its frequency-dependent electric field of THz signal transmitted through the sample $S_{sample}(\omega)$ and empty cuvette $S_{ref}(\omega)$ is written as $^{32-37}$

$$S_{sample}(\omega) = t_{quartz \to sample} p_{sample} t_{sample \to quartz} E(\omega)$$
 (1)

$$S_{ref}(\omega) = t_{quartz \to air} P_{air} t_{air \to quartz} E(\omega), \tag{2}$$

where $E(\omega)$ is the incident THz electric field, $t_{a \to b} \left(= \frac{2 \tilde{n}_b}{\tilde{n}_a + \tilde{n}_b} \right)$ is Fresnel's transmission coefficient from medium a to medium b and $p_a (= \exp \left[-i \left(\tilde{n}_a \right) \frac{\omega L}{c} \right])$ is propagation coefficient in medium over a distance L, with the complex refractive index represented by $\tilde{n}_a(\omega) = n_a(\omega) + i k_a(\omega)$ where $n_a(\omega)$ and $k_a(\omega)$ are real and imaginary part of the complex refractive index of medium a and c is the speed of light. The frequency-dependent complex transmission coefficient $T(\omega)$ is given by

$$T(\omega) = \frac{S_{\text{sample}}(\omega)}{S_{\text{ref}}(\omega)} = \frac{\widetilde{n}_{\text{sample}}(\omega) \left(1 + \widetilde{n}_{\text{quartz}}(\omega)\right)^{2}}{\left(\widetilde{n}_{\text{sample}}(\omega) + \widetilde{n}_{\text{quartz}}(\omega)\right)^{2}} \exp\left[-i\left(\widetilde{n}_{\text{sample}}(\omega) - 1\right) \frac{\omega L}{c}\right]$$
(3)

where $\widetilde{n}_{sample}(\omega)$ and $\widetilde{n}_{quartz}(\omega)$ are the complex refractive indices of the sample and quartz cuvette window, respectively. The power absorption coefficient was estimated as $\alpha(\omega) = k(\omega)4\pi/\lambda$ with the wavelength λ . Additionally, the complex dielectric permittivity $\widetilde{\epsilon}$ is calculated as $\widetilde{\epsilon}(\omega) = \varepsilon_{real}(\omega) + i\varepsilon_{imag}(\omega) = (\widetilde{n}(\omega))^2$. Equation 3 was solved using a numerical method in MATLAB³².

Data Availability

No datasets were generated or analysed during the current study.

Received: 10 April 2025; Accepted: 21 June 2025;

Published online: 17 July 2025

References

- Asif, M. Health effects of omega-3,6,9 fatty acids: Perilla frutescens is a good example of plant oils. Orient Pharm. Exp. Med. 11, 51–59 (2011).
- 2. Lands, W. E. M. Fish, Omega-3 and Human Health. (AOCS Press, 2005).
- Bischoff-Ferrari, H. A. et al. Individual and additive effects of vitamin D, omega-3 and exercise on DNA methylation clocks of biological aging in older adults from the DO-HEALTH trial. Nat. Aging 5, 376–385 (2025).
- 4. Shin, H.-S. Perilla: The Genus Perilla. (CRC Press, 1997).
- Guillén, M. D. & Ruiz, A. 1H nuclear magnetic resonance as a fast tool for determining the composition of acyl chains in acylglycerol mixtures. *Eur. J. Lipid Sci. Technol.* 105, 502–507 (2003).
- Castejón, D., Mateos-Aparicio, I., Molero, M. D., Cambero, M. I. & Herrera, A. Evaluation and optimization of the analysis of fatty acid types in edible oils by 1H-NMR. Food Anal. Methods 7, 1285–1297 (2014).
- Ye, Q. & Meng, X. Highly efficient authentication of edible oils by FTIR spectroscopy coupled with chemometrics. Food Chem. 385, 132661 (2022).
- Vongsvivut, J., Miller, M. R., McNaughton, D., Heraud, P. & Barrow, C. J. Rapid discrimination and determination of polyunsaturated fatty acid composition in marine oils by FTIR spectroscopy and multivariate data analysis. *Food Bioproc. Tech* 7, 2410–2422 (2014).
- Hong, S. J. et al. Rancidity estimation of perilla seed oil by using nearinfrared spectroscopy and multivariate analysis techniques. *J. Spectrosc.* 2017, 1 (2017).
- Maeng, I. et al. Unique phonon modes of a CH3NH3PbBr3 hybrid perovskite film without the influence of defect structures: an attempt toward a novel THz-based application. NPG Asia Mater. 12, 53 (2020).
- Lee, S. H. et al. Graphene assisted terahertz metamaterials for sensitive bio-sensing. Sens. Actuators B Chem. 310, 127841 (2020).
- Shin, H. J., Choi, S. W. & Ok, G. Qualitative identification of food materials by complex refractive index mapping in the terahertz range. Food Chem. 245, 282–288 (2018).
- Shin, H. J., Lim, J. H., Park, K. J. & Ok, G. State-of-the-art nondestructive high-speed raster scanning inspection for food safety and quality using terahertz refractive index mapping. *Food Chem.* Adv. 4, 100685 (2024).
- Lee, S. H., Lee, D., Choi, M. H., Son, J. H. & Seo, M. Highly sensitive and selective detection of steroid hormones using terahertz moleculespecific sensors. *Anal. Chem.* 91, 6844–6849 (2019).
- 15. Oh, S. J., Son, J. H., Yoo, O. & Lee, D. H. Terahertz characteristics of electrolytes in aqueous Luria-Bertani media. *J. Appl. Phys.* **102**, 074702 (2007).
- Lee, D. K. et al. Highly sensitive and selective sugar detection by terahertz nano-antennas. Sci. Rep. 5, 15459 (2015).
- Oh, S. J. et al. Measurement depth enhancement in terahertz imaging of biological tissues. Opt. Express 21, 21299 (2013).
- Brucherseifer, M. et al. Label-free probing of the binding state of DNA by time-domain terahertz sensing. Appl Phys. Lett. 77, 4049–4051 (2000).
- Shin, H. J., Oh, S. J., Kim, S. I., Won Kim, H. & Son, J. H. Conformational characteristics of B -glucan in laminarin probed by terahertz spectroscopy. *Appl. Phys. Lett.* 94, 111911 (2009).
- Kindt, J. T. & Schmuttenmaer, C. A. Far-Infrared Dielectric Properties of Polar Liquids Probed by Femtosecond Terahertz Pulse Spectroscopy. *J. Phys. Chem.* 100, 10373–10379 (1996).
- Pedersen, J. E. & Keiding, S. R. THz Time-Domain Spectroscopy of Nonpolar Liquids. *IEEE J. Quantum Electron.* 28, 2518–2522 (1992).
- Jin, Y.-S., Kim, G.-J., Shon, C.-H., Jeon, S.-G. & Kim, J.-I. Analysis of petroleum products and their mixtures by using terahertz time domain spectroscopy. *J. Korean Phys. Soc.* 53, 1879–1885 (2008).
- Abdul-Munaim, A. M., Ornik, J., Koch, M. & Watson, D. G. Terahertz time domain spectroscopy to detect different oxidation levels of diesel engine oil. *Lubricants* 7, 18 (2019).
- 24. Nishimura, N., Ogura, R., Matsumoto, S., Mizuno, M. & Fukunaga, K. Study of molecular behavior in oxidation of insulating oil using

- terahertz spectroscopy. *Electr. Eng. Jpn. (Engl. translation Denki Gakkai Ronbunshi)* **183**, 9–15 (2013).
- Adbul-Munaim, A. M., Reuter, M., Koch, M. & Watson, D. G. Distinguishing gasoline engine oils of different viscosities using terahertz time-domain spectroscopy. *J. Infrared Millim. Terahertz* Waves 36, 687–696 (2015).
- Dinovitser, A., Valchev, D. G. & Abbott, D. Terahertz time-domain spectroscopy of edible oils. R. Soc. Open Sci. 4, 170275 (2017).
- 27. Karaliūnas, M. et al. Non-destructive inspection of food and technical oils by terahertz spectroscopy. *Sci. Rep.* **8**, 18025 (2018).
- Gorenflo, S. et al. Dielectric properties of oil-water complexes using terahertz transmission spectroscopy. *Chem. Phys. Lett.* 421, 494–498 (2006).
- Abdul-Munaim, M. et al. Using terahertz time-domain spectroscopy to discriminate among water contamination levels in diesel engine oil. *Trans. ASABE* 59, 795–801 (2016).
- 30. United States Department of Agriculture. Corn oil, industrial and retail, all purpose salad or cooking, fat composition, 100 g. https://fdc.nal.usda.gov/food-details/171029/nutrients (2019).
- United States Department of Agriculture. Soybean oil, salad or cooking, fat composition, 100 g. https://fdc.nal.usda.gov/fooddetails/171411/nutrients (2019).
- Duvillaret, L., Garet, F. & Coutaz, J.-L. A Reliable Method for Extraction of Material Parameters in Terahertz Time-Domain Spectroscopy. *IEEE J. Sel. Top. Quantum Electron.* 2, 739–746 (1996).
- Duvillaret, L., Dé, F., Garet, R. & Coutaz, J.-L. Highly Precise Determination of Optical Constants and Sample Thickness in Terahertz Time-Domain Spectroscopy. Appl Opt. 38, 409–415 (1999).
- Dorney, T. D., Baraniuk, R. G. & Mittleman, D. M. Material Parameter Estimation with Terahertz Time-Domain Spectroscopy. J. Opt. Soc. Am. A Opt. Image Sci. Vis. 18, 1562–1571 (2001).
- Choi, J., Kwon, W. S., Kim, K. S. & Kim, S. Nondestructive Material Characterization in the Terahertz Band by Selective Extraction of Sample-Induced Echo Signals. *J. Nondestr Eval.* 34, 269 (2015).
- Mukherjee, S., Kumar, N. M. A., Upadhya, P. C. & Kamaraju, N. A review on numerical methods for thickness determination in terahertz timedomain spectroscopy. *Eur. Phys. J.: Spec. Top.* 230, 4099–4111 (2021).
- 37. Weisenstein, C. et al. THz Detection of Biomolecules in Aqueous Environments—Status and Perspectives for Analysis Under Physiological Conditions and Clinical use. *J. Infrared, Millim., Terahertz Waves* **42**, 607–646 (2021).

Acknowledgements

This work was financially supported by the National Research Foundation (NRF) grant (No. RS-2024-00454894 and RS-2024-00348608) funded by the Ministry of Science and ICT (MSIT) of the Korean government. Additional support was provided by the fs-THz beamline at Pohang Accelerator Laboratory.

Author contributions

L.-H.Y. writing—original draft; L.-H.Y., Y.B.J., and H.B. investigation; I.M. data curation and visualization; H.J.S. Conceptualization; S.L. and K.K. Methodology; S.J.Oh. editing and supervision.

Competing interests

The authors declare no competing interests.

Additional information

Correspondence and requests for materials should be addressed to Hee Jun Shin or Seung Jae Oh.

Reprints and permissions information is available at

http://www.nature.com/reprints

Publisher's note Springer Nature remains neutral with regard to jurisdictional claims in published maps and institutional affiliations.

Open Access This article is licensed under a Creative Commons Attribution-NonCommercial-NoDerivatives 4.0 International License, which permits any non-commercial use, sharing, distribution and reproduction in any medium or format, as long as you give appropriate credit to the original author(s) and the source, provide a link to the Creative Commons licence, and indicate if you modified the licensed material. You do not have permission under this licence to share adapted material derived from this article or parts of it. The images or other third party material in this article are included in the article's Creative Commons licence, unless indicated otherwise in a credit line to the material. If material is not included in the article's Creative Commons licence and your intended use is not permitted by statutory regulation or exceeds the permitted use, you will need to obtain permission directly from the copyright holder. To view a copy of this licence, visit http://creativecommons.org/licenses/by-nc-nd/4.0/.

© The Author(s) 2025